JOURNAL OF MAGNETIC RESONANCE **135,** 216–226 (1998)
ARTICLE NO. MN981545

New Methylene Specific Experiments for the Measurement of Scalar Spin–Spin Coupling Constants between Protons Attached to ^{13}C

T. Carlomagno, H. Schwalbe, A. Rexroth, O. W. Sørensen,* and C. Griesinger[1]

*Institut für Organische Chemie, Universität Frankfurt, Marie-Curie Strasse 11, D-60439 Frankfurt/Main, Germany; and *Department of Chemistry, Carlsberg Laboratory, Gamle Carlsberg Vej 10, DK-2500 Valby, Denmark*

E-mail: cigr@krypton.org.chemie.uni-frankfurt.de

Received May 1, 1998

New two- and three-dimensional NMR methods are proposed for the measurement of ^3J(H, H) coupling constants between two adjacent methylene moieties. The new experiment, which is based on a combination of the E.COSY principle and double/zero quantum heteronuclear spectroscopy, has been applied to diacetonglucose and to the protein rhodniin. The coupling constants of CH-CH_2 groups have been compared with those obtained from a HCCH-E.COSY experiment to check the reliability of the results. An analysis of the coupling constants derived by comparison between experimental and simulated spectra is presented. Simulations were done with the program wtest considering fully correlated dipolar relaxation. Side-chain conformations in amino acids with adjacent methylene groups can be determined by the new experiment.

Key Words: **E.COSY; DQ/ZQ-HCCH-E.COSY; multiple quantum spectroscopy; vicinal proton coupling constant; data simulation; auto-correlated and cross-correlated relaxation.**

INTRODUCTION

Knowing the local conformation of amino acid side-chains can be of importance in understanding protein function involving side-chain/side-chain interactions. Whereas the side-chain angle χ_n can be obtained from ^3J heteronuclear couplings, the stereospecific assignment of protons in CH_2-CH_2 moieties can be achieved only via homonuclear ^3J proton–proton couplings (*1–3*). Many techniques have been introduced in the last years to obtain ^3J(H,H) couplings in biomolecules with different labelling pattern. In ^{13}C-labeled molecules H,H coupling constants can be determined via the HCCH-E.COSY (*4–9, 14*) method. The E.COSY type experiments (*10–12*) rely on the correlation of two active nuclei k and l, which are both scalar coupled to a third nucleus m. In order to get the typical two-dimensional E.COSY multiplet pattern the state of the spin m must not be perturbed after the evolution of the first of the two couplings $J(k,m)$ and $J(l,m)$. For the HCCH-E.COSY experiment in an H^1C^1-C^2H^3(H) moiety, the passive spin m is H^1, and the active spins k and l are C^1 and H^3 in ω_1 and ω_2, respectively. The multiplet is split by $^1J(C^1,H^1)$ in ω_1 and the coupling of interest $^3J(H^1,H^3)$ in ω_2, as shown in Fig. 1a. The HCCH-E.COSY experiment works well for CH_n-CH_m moieties, except for n = m = 2. For a $H^1H^2C^1$-$C^2H^3(H)^2$ moiety, excitation of inphase C^1 single-quantum coherence during t_1 leads to a quadruplet in ω_1 with severe overlap of the two inner lines (Fig. 1b); from this multiplet structure it is possible to determine only the sum of the two $^3J(H^1,H^3)$ and $^3J(H^2,H^3)$ coupling constants in ω_2. In Ref. (*5*), an experimental approach for the unambiguous determination of the four ^3J(H,H) coupling constants in CH_2-CH_2 groups was introduced. The scheme requires the combination of one 3D and two 2D spectra and is therefore rather complicated and time-consuming.

In the first part of this paper we introduce a new NMR technique, the DQ/ZQ-HCCH-E.COSY, that relies on an E.COSY-type correlation (*10–12*) between heteronuclear double/zero quantum (DQ/ZQ) coherences (*13*) of one of the CH_2 groups and proton coherence of the other CH_2 group. The method allows direct measurement of the four ^3J(H,H) coupling constants in CH_2-CH_2 segments without any post-acquisition linear combination of data obtained from two different experiments. The principle of the technique will be demonstrated on the CH_2-CH moiety of diaceton-glucose (Fig. 2); the analysis of coupling constants in side-chains with several adjacent methylene groups will be shown on a proline ring of the protein rhodniin.

In the second part of the paper we present an analysis of the coupling constants in CH-CH_2 segments extracted from both the HCCH-E.COSY experiment and from the new DQ/ZQ-HCCH-E.COSY experiment. For fast relaxing macromolecules with high spin densities we demonstrate the need for a more sophisticated procedure of data analysis than that based on the measurement of the shift of the two components of the cross peak. In this respect, we suggest the fitting of experimental data with simulated spectra, that are calculated taking fully correlated dipolar relaxation into account.

[1] To whom correspondence should be addressed.

[2] Whether the detected proton H^3 belongs to a methylene group or to a methine group is irrelevant.

1090-7807/98 $25.00

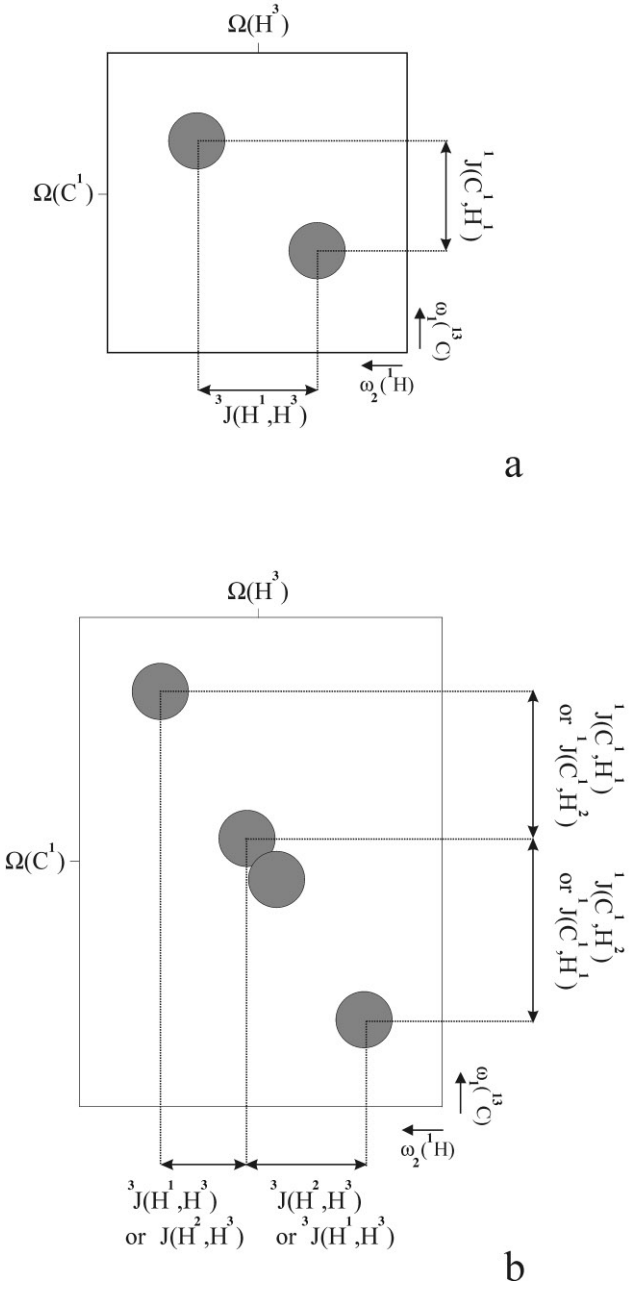

FIG. 1. Schematic representation of the cross peaks obtained in a 2D HCCH-E.COSY spectrum for a H^1C^1-C^2H^3(H) moiety (a) and for a $H^1H^2C^1$-C^2H^3(H) moiety (b). In both cases carbon C^1 magnetization evolves during t_1 and the proton H^3 is detected during acquisition. The multiplet in (a) shows only two components, the relative shift of which in ω_2 gives the desired $^3J(H^1,H^3)$ coupling; the multiplet in (b) consists of four components with a partial overlap of the two inner ones: due to this overlap only the sum of $^3J(H^1,H^3)$ and $^3J(H^2,H^3)$ can be determined.

THEORY

Let us consider the $H^1H^2C^1$-C^2H^3 group of diaceton-glucose. If C^2 coherence is excited during t_1, the classical HCCH-E.COSY experiment (*4*, *5*) can be used to determine the $^3J(H^1, H^3)$ and $^3J(H^2,H^3)$ coupling constants ($k = C^2$; $l = H^1$ or H^2; $m = H^3$). However, if C^1 magnetization is excited in t_1, only the sum of the two $^3J(H,H)$ can be obtained with the standard HCCH-E.COSY technique ($k = C^1$; $l = H^3$; $m = H^1$; $p = H^2$). The effect of the coupling of C^1 to the second passive proton H^2 can be eliminated by exciting DQ/ZQ coherences of H^2 and C^1, since they commute with $J(C^1,H^2)$. The pulse sequence is shown in Fig. 3, together with the product operator description, while the schematic multiplet pattern is shown in Fig. 4. Several implementations of the 2D DQ/ZQ-HCCH-E.COSY experiment are possible, which differ in the evolution times of the H^2 and C^1 chemical shifts as well as of the $^2J(H^1, H^2)$ and $^1J(C^1,H^1)$ couplings. The implementation shown in Fig. 3 was chosen according to two different criteria: first, the combination of the evolution times of the H^2 and C^1 chemical shifts and of the $^1J(C^1,H^1)$ coupling has to allow sufficient mutual separation of the H^2C^1-H^3 and H^1C^1-H^3 peaks; second, since the evolution of the $^2J(H^1,H^2)$ coupling from proton excitation to before point (1) causes a phase difference in ω_1 of the two doublet components with different polarization state of the passive proton, it is advisable to keep this period as short as possible, in order to get easily phaseable doublets. Excitation of H^2C^1-DQ/ZQ quantum coherence leads to a doublet in ω_1 due to the zero coupling $aJ(H^1,H^2) \pm bJ(C^1,H^1)$, where a and b are two numerical factors depending on the effective evolution time of $^2J(H^1,H^2)$ and $^1J(C^1,H^1)$ (for the sequence in Fig. 3, $a = 5/2$ and $b = -1$). The transfer of the DQ/ZQ coherence to H^3, without changing the spin state of H^1 (passive spin), leads to an E.COSY type multiplet pattern, from which the desired $^3J(H^1, H^3)$ can be extracted (Fig. 4). The coherence transfer pathway comprises H^2, C^1 DQ/ZQ excitation and transfer of coherence from C^1 to C^2 and from C^2 to H^3. The key steps are

$$2C_{1y}H_{2x}H_{1\alpha,\beta} \xrightarrow{1} 2C_{1y}H_{2z}H_{1\alpha,\beta} \xrightarrow{2}$$

$$2C_{1y}C_{2z}H_{1\alpha,\beta} \xrightarrow{3} 2C_{2y}H_{3z}H_{1\alpha,\beta} \xrightarrow{4} H_{3x}H_{1\alpha,\beta}.$$

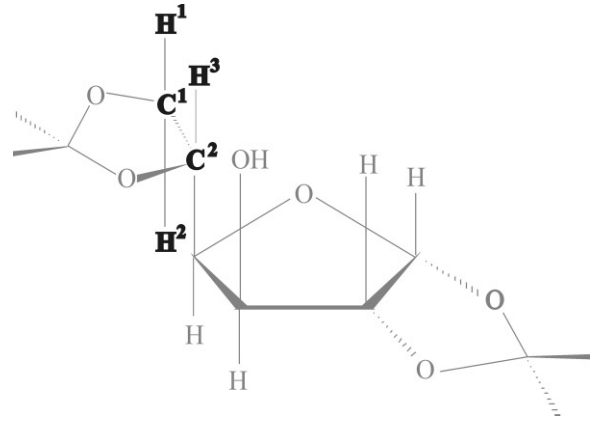

FIG. 2. Structure of diaceton-glucose. The atoms in bold represent the $H^1H^2C^1$-C^2H^3 moiety used as test for the DQ/ZQ-HCCH-E.COSY sequence.

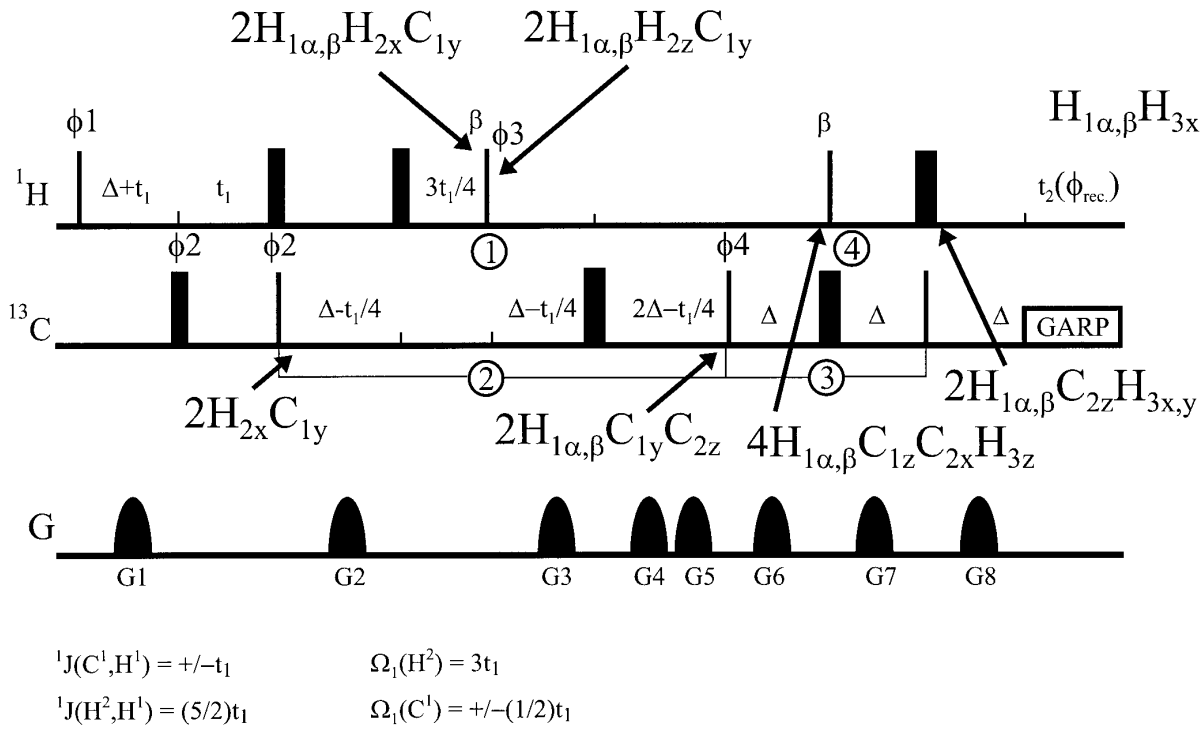

$^1J(C^1,H^1) = +/-t_1$ $\quad\quad$ $\Omega_1(H^2) = 3t_1$

$^1J(H^2,H^1) = (5/2)t_1$ $\quad\quad$ $\Omega_1(C^1) = +/-(1/2)t_1$

FIG. 3. The 2D DQ/ZQ-HCCH-E.COSY pulse sequence with product operator description of the magnetization transfer pathway in a $H^1H^2C^1$-C^2H^3 moiety $\beta = 54.7°$; $\Delta = 3.3$ ms [$\approx 1/(2J(H,C))$]; $\phi1 = x, -x$; $\phi2 = 2x, 2(-x)$; $\phi3 = y$; $\phi4 = 4x, 4(-x)$; $\phi_{rec.} = x, -x, -x, x$. Pure DQ and ZQ coherences in ω_1 are obtained by subtracting and adding respectively two FIDs acquired with phases ($\phi1$, $\phi2$) and ($\phi1 + 90°$, $\phi2 + 90°$). Quadrature detection is achieved by incrementing either $\phi1$ or $\phi2$ by 90° (States-TPPI). The gradients are chosen according to the following conditions: G1 = G2; G2 + G3 = G4 + G5; G6 = G7 = G8.

Steps 2 and 3 are afforded by evolution of couplings and carbon pulses only, whereas steps 1 and 4 require also proton pulses. To obtain the E.COSY type pattern, the proton pulses required for transfers 1 and 4 need to be optimized to conserve at the end of the sequence the initial state of spin H^1 and to obtain optimal transfer of $H_{2x} \xrightarrow{1} H_{2z}$ and $H_{3z} \xrightarrow{4} H_{3x}$. Two transfer pathways are possible,

$$\text{(a) } 2C_{1y}H_{2x}H_{1\alpha} \xrightarrow{1:\beta(H)} 2C_{1y}H_{2z}H_{1\alpha} \xrightarrow{2,3} 2C_{2y}H_{3z}H_{1\alpha} \xrightarrow{4:\beta'(H)} H_{3x}H_{1\alpha}$$

with amplitude equal to $\sin\beta\sin\beta'\cos^2(\beta/2)\cos^2(\beta'/2)$, and

$$\text{(b) } 2C_{1y}H_{2x}H_{1\alpha} \xrightarrow{1:\beta(H)} 2C_{1y}H_{2z}H_{1\beta} \xrightarrow{2,3} 2C_{2y}H_{3z}H_{1\beta} \xrightarrow{4:\beta'(H)} H_{3x}H_{1\alpha}$$

with amplitude equal to $\sin\beta\sin\beta'\sin^2(\beta/2)\sin^2(\beta'/2)$, while the following two transfers need to be suppressed,

$$\text{(c) } 2C_{1y}H_{2x}H_{1\alpha} \xrightarrow{1:\beta(H)} 2C_{1y}H_{2z}H_{1\beta} \xrightarrow{2,3} 2C_{2y}H_{3z}H_{1\beta} \xrightarrow{4:\beta'(H)} H_{3x}H_{1\beta}$$

with amplitude equal to $\sin\beta\sin\beta'\sin^2(\beta/2)\cos^2(\beta'/2)$, and

$$\text{(d) } 2C_{1y}H_{2x}H_{1\alpha} \xrightarrow{1:\beta(H)} 2C_{1y}H_{2z}H_{1\alpha} \xrightarrow{2,3} 2C_{2y}H_{3z}H_{1\alpha} \xrightarrow{4:\beta'(H)} H_{3x}H_{1\beta}$$

with amplitude equal to $\sin\beta\sin\beta'\cos^2(\beta/2)\sin^2(\beta'/2)$.

Pathways (c) and (d) could be easily suppressed if it is possible to create destructive interference between them. This is indeed possible if, after transfer 1, the operators evolve

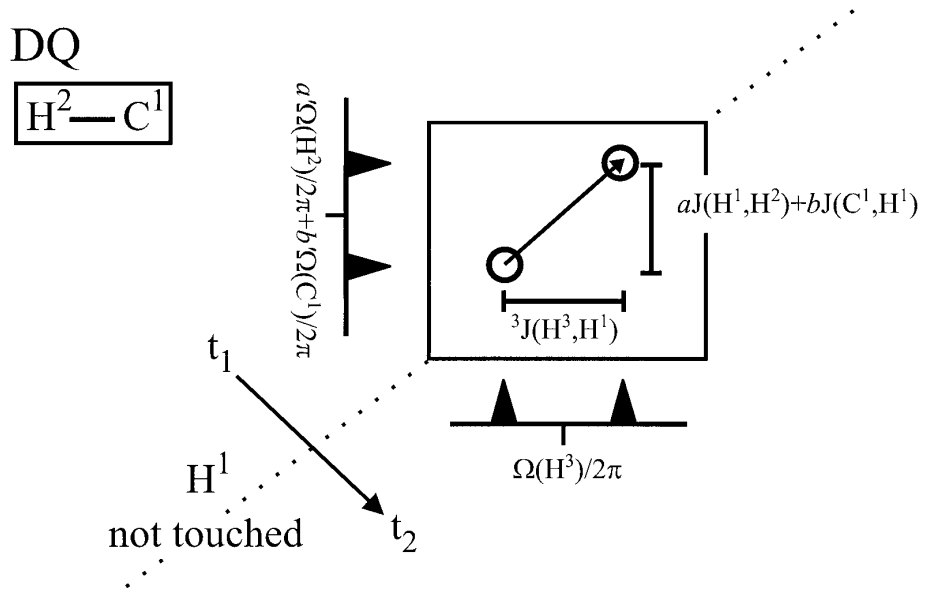

FIG. 4. Schematic representation of the DQ cross peak obtained for a $H^1H^2C^1$-C^2H^3 moiety with the sequence of Fig. 3. The coefficient a and b are equivalent to the number of t_1 times during which the couplings $^2J(H^1,H^2)$ and $^1J(C^1,H^1)$ evolve, respectively (for the sequence of Fig. 3, $a = 5/2$ and $b = -1$); the coefficients a' and b' are equivalent to the number of t_1 times during which the chemical shifts of H^2 and C^1 evolve respectively (for the sequence of Fig. 3, $a' = 3$ and $b' = 1/2$). The desired $^3J(H^1,H^3)$ coupling can be determined from the relative shift in ω_2 of the two components of the multiplet.

heteronuclear coupling during $(2J)^{-1} = (2\ ^1J_{CH})^{-1}$. This leads to the following transfer amplitudes:

$$2C_{1y}H_{2z}H_{1\alpha} \xrightarrow{(2J)^{-1}} -C_{1y}H_{1\alpha}$$

$$2C_{1y}H_{2z}H_{1\beta} \xrightarrow{(2J)^{-1}} C_{1y}H_{1\beta}.$$

Pathways (c) and (d) have opposite phase and therefore cancel each other automatically, provided $\beta = \beta'$. The desired transfers (a) and (b) can be optimized maximizing the expression

$$\sin^2\beta\cos^4(\beta/2) - \sin^2\beta\sin^4(\beta/2) = \sin^2\beta\cos\beta.$$

The minus sign comes from the fact that the two pathways (a) and (b), in analogy to (c) and (d), develop opposite phases due to the $(2J)^{-1}$ delay. The optimal flip angle is the magic angle $\beta = \text{arctg}(\sqrt{2}) = 54.7°$, which was also found in another similar experiment with respect to a passive spin (*15*).

Transfer 1 is effected by a β(H) pulse; transfer 4 is effected by a β(H) pulse plus a 90°(C) pulse and a refocussing delay of duration $\Delta = (2^1J_{C,H})^{-1}$. The ^{13}C,^{13}C transfer is obtained by a normal relayed transfer step. The coherence transfer from C^2 to H^3 is done via a DEPT-type sequence (*14*). In the sequence of Fig. 3 the proton chemical shift evolves for $3t_1$; the carbon chemical shift evolves only for $0.5t_1$.

The two peaks of the E.COSY multiplet have different phases both in ω_1 ($e^{i2\pi J(H^1H^2)\Delta}$ for the peak associated with the H^1_α state and $e^{-i2\pi J(H^1H^2)\Delta}$ for the peak associated with the H^1_β state) and in ω_2 ($e^{i2\pi J(H^1H^3)\Delta}$ for the peak associated with the H^1_α state and $e^{-i2\pi J(H^1H^3)\Delta}$ for the peak associated with the H^1_β state). While the phase difference in ω_1 does not affect the measurement of the $J(H^1,H^3)$, the phase difference in ω_2 has to be corrected for before extracting coupling constants. Since the necessary correction depends on the desired J value, an iterative procedure has to be applied, as explained later. Gradients are used whenever possible in the pulse sequence to suppress artifacts, unwanted coherence pathways and the effect of pulse imperfections.

The DQ or the ZQ spectrum can be obtained with the sequence shown in Fig. 3 by an appropriate combination of experiments acquired with different ϕ_1 and ϕ_2 phases, as explained in the figure caption.

The presence of heteronuclear DQ and ZQ coherences in an evolution period where ^{13}C chemical shifts and J(C, H) evolve is crucial for the new technique but for the multiplet structure it is irrelevant whether or not ^1H chemical shifts are refocused during that period. ^1H chemical-shift evolution is however necessary for separation of the two peaks associated with H^1C^1 and H^2C^1, respectively. This labeling with ^1H chemical shifts can occur in another evolution period, as, for example, in the 3D version of the experiment (Fig. 5a). Here evolution of ^1H chemical shifts occurs in t_2, while the ^{13}C chemical shifts evolve in t_1. The E.COSY-type multiplet is obtained in ω_1-ω_3 planes. The two peaks of the multiplet have different phases in ω_2 and ω_3, as for the 2D version of the experiment ($e^{i4\pi J(H^1H^2)\Delta}$ in ω_1 and $e^{i2\pi J(H^1H^3)\Delta}$ in ω_3 for the peak associated with the H^1_α state and $e^{-i4\pi J(H^1H^2)\Delta}$ in ω_1 and $e^{-i2\pi J(H^1H^3)\Delta}$ in ω_3 for the peak associated with H^1_β state).

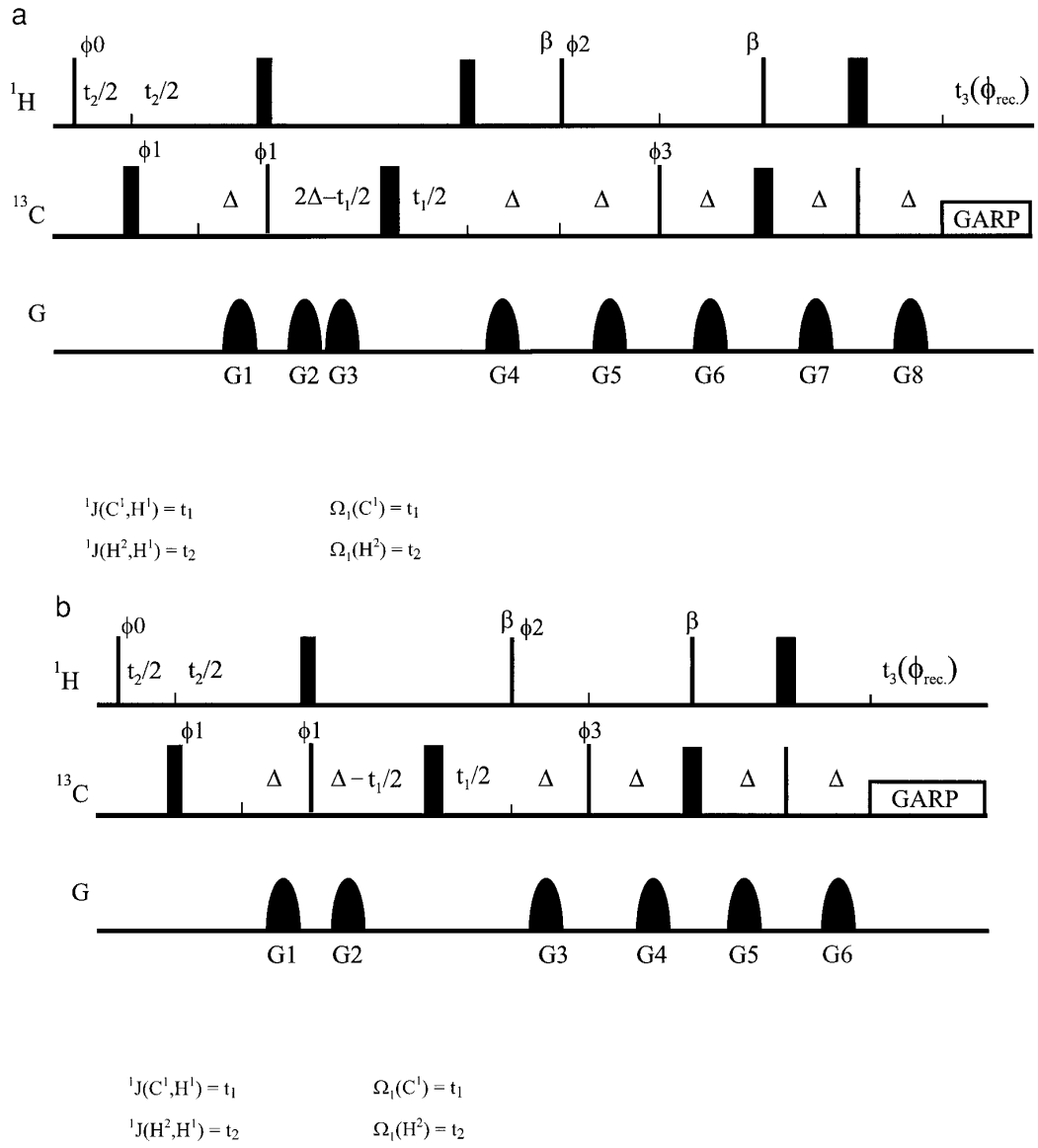

FIG. 5. The 3D DQ/ZQ HCCH-E.COSY pulse sequence. $\beta = 54.7°$; $\Delta = 3.57$ ms $[\approx(2^1J_{C,H})^{-1}]$; $\phi0 = x$; $\phi1 = x, -x$; $\phi2 = y$; $\phi3 = 2x, 2(-x)$; $\phi_{rec.} = x, -x$. The chemical shifts of the two spins constituting the DQ/ZQ terms are recorded separately: for a $H^1H^2C^1$-C^2H^3 moiety, where H^1 is the passive spin, $\omega(C^1)$ is registered in ω_1, $\omega(H^2)$ is registered in ω_2, and $\omega(H^3)$ is in ω_3. Therefore no separation of the DQ and ZQ terms is necessary. States-TPPI is applied individually for $\phi0$ and $\phi1$. The desired $^3J(H^1,H^3)$ coupling is derived from the relative shift of the two components of the multiplet in the ω_3 dimension of the ω_1-ω_3 plane. (a) Optimized version for magnetization starting on a CH_n moiety where the carbon is bound to only one other carbon (total evolution time of $^1J_{C,C}$ $4\Delta = (2^1J_{C,C})^{-1}$ before the C,C relay step); the gradients follow the conditions G1 + G4 = G2 + G3; G2 + G3 = G4 + G5; G6 = G7 = G8.; (b) general version for magnetization starting on CH_n groups with carbon bound to both one and two other carbons (total evolution time of $^1J_{C,C}$ $2\Delta = (4^1J_{C,C})^{-1}$ before the C,C relay step); the gradients follow the conditions G1 = G2 = G3; G4 = G5 = G6.

EXPERIMENTAL AND RESULTS

The multiplets resulting from the application of the DQ/ZQ-HCCH-E.COSY sequence reported in Fig. 3 to diaceton-glucose are shown in Fig. 6 for the double-quantum spectrum. Both the peaks, originating from the $H^1 \rightarrow H^3$ and $H^2 \rightarrow H^3$ transfers, are observable. From these peaks it is possible to derive the two couplings $^3J(H^1,H^3)$ and $^3J(H^2,H^3)$, respectively, as shown in the figure. Similar results are found in the zero-quantum spectrum and are identical to coupling constants measured in ^{1}H spectra.

The 3D version of the experiment in Fig. 5a is optimized for transfer starting on a methylene carbon which is coupled to only one other carbon. In fact the $^1J_{C,C}$ coupling evolves for $4\Delta = (2^1J_{C,C})^{-1}$, instead of $(4^1J_{C,C})^{-1}$, which would deliver maximum transfer for a carbon which is coupled to two other carbons and about 70% of the maximum intensity for transfer from a carbon which is coupled to only one other

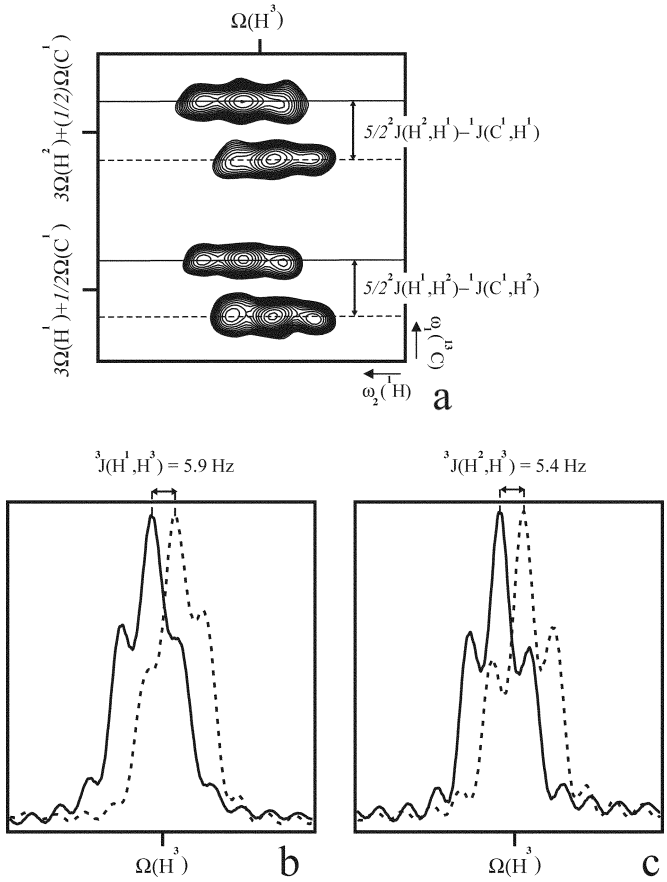

FIG. 6. In (a) the DQ spectrum acquired with the sequence of Fig. 3 on a chloroform solution of diaceton-glucose is shown. The spectrum was recorded at 300 K on a Bruker AMX 600 spectrometer. Both peaks deriving from the $H^1H^2C^1$-C^2H^3 moiety, shown in bold in Fig. 2, are present. The axis values are reported next to each peak. The spectral widths were 16000 Hz (ω_1) and 7250 Hz (ω_2) and the acquired matrix 180(t_1) × 2048(t_2); the number of complex points in t_1 was extended to 320 by linear prediction; both dimensions were zero-filled to 8K complex points. The number of scans was 16. The strengths and lengths of the gradients were G1 = 21 G/cm, 1ms; G2 = G3 = G4 = G5 = G6 = 12 G/cm, 200μs. (b) ω_2 traces extracted from the upper peak of the 2D spectrum along the indicated lines: the $^3J(H^1,H^3)$ can be measured from the relative shift of the two sub-multiplets in ω_2, as indicated; (c) ω_2 traces extracted from the lower peak of the 2D spectrum along the indicated lines: the $^3J(H^2,H^3)$ coupling is derived from the relative shift of the two sub-multiplets in ω_2. The values for the two desired coupling constants are $^3J(H^1,H^3) = 5.9$ Hz and $^3J(H^2,H^3) = 5.4$ Hz.

carbon. The more general version of the sequence is given in Fig. 5b. The experimental parameters are reported in the figure caption. To check the reliability of the method the $^3J(H^\alpha,H^\beta)$ and $^3J(H^\alpha,H^{\beta'})$ coupling constants of aspartatic acid, asparagine, phenylalanine, tyrosine, serine, and cysteine residues of the protein rhodniin, extracted from the DQ/ZQ-HCCH-E.COSY experiment, have been compared to those derived from a previously acquired HCCH-E.COSY experiment. The extraction of the coupling constants was performed with both of the following procedures: (a) measuring the frequency shift which was necessary to apply to one of the two components of the multiplet to obtain maximum overlap with the other one: the quality of the overlap was judged by visual inspection; (b) finding, with an automated procedure, the ^3J(H, H) that gives a minimum for the integral of the power difference spectrum between the two traces of the multiplet shifted by the trial J-coupling (*6*). The automated procedure could not always be applied due to either overlap of the interesting signals or low signal-to-noise ratio. When both methods were applicable, they gave comparable results; therefore from now on we will refer to the values obtained with the first procedure and we will call these values apparent coupling constants J^{exp}_{app}. In the HCCH-E.COSY experiment the incomplete suppression of the non-connected transitions was corrected by the method described in Ref. (*6*). Owing to the evolution of the desired ^3J(H, H) coupling before acquisition the phase of the two traces of the multiplet is not identical. Therefore an iterative procedure was carried out, which consisted in measuring the ^3J(H, H) coupling and applying the corresponding frequency dependent phase correction until convergence was reached. The values for the six best behaving residues, namely those showing well separated, relatively intense peaks in both spectra, are reported in the first and fourth columns of Table 1. The coupling constants extracted from the HCCH-E.COSY experiment (first column) are systematically lower than those extracted from the DQ/ZQ-HCCH-E.COSY spectrum (fourth column). This observation points to the need for a more detailed analysis of the multiplets in both experiments and to a deeper understanding of the intrinsic sources of error of each method.

SIMULATION

One major drawback of the procedures mentioned above for the extraction of coupling constants from E.COSY-type experiments is the fact that relaxation effects, present both during acquisition and during the whole sequence, introduce non-identical sub-multiplet patterns for the two spin states of the passive spin (*9*). As can be seen in Fig. 7 for S89, in the HCCH-E.COSY spectrum, where the two traces are doublets due to the $^2J(H^\beta,H^{\beta'})$ coupling, the outer lines appear to be considerably weaker than the inner ones (Fig. 7a); in the DQ/ZQ-HCCH-E.COSY spectrum, the α and β components of the multiplet have an apparently different coupling topology: one seems to be a triplet while the other is closer to a quartet (Fig. 7b). These peculiar characteristics of the lineshape make the extraction of coupling constants rather difficult. Therefore, we tried to improve the extraction procedure by fitting experimental lines to simulated ones, taking both couplings and relaxation into account. The theoretical multiplets for a $H^1H^2C^1$-C^2H^3 unit in both the HCCH-E.COSY and in the DQ/ZQ-HCCH-E.COSY experiment were obtained with the simulation program wtest (*17*). In both cases the simulations included the whole pulse sequence and started with ^{1}H magnetization of the CH group

TABLE 1
Values of Apparent Experimental and Simulated *J* and of Best Fit *J* for Both HCCH-E.COSY and DQ/ZQ-HCCH-E.COSY Experiments

	$J(H^{\alpha}, H^{\beta})$, $J(H^{\alpha}, H^{\beta'})$					
	HCCH-E.COSY			DQ/ZQ-HCCH-E.COSY		
Residue	J_{app}^{exp} (Hz)	J_{app}^{sim} (Hz)	J_{opt} (Hz)	J_{app}^{exp} (Hz)	J_{app}^{sim} (Hz)	J_{opt} (Hz)
C69	1.3, 9.0	1.5, 10.0	4.4, 12.6	5.6, 11.3	5.4, 11.5	5.7, 11.4
D72	0.8, 1.3	0.3, 0.8	2.5, 3.1	2.9, 2.3	2.8, 2.2	3.0, 2.3
D73	3.8,/	4.3,/	5.9,/	5.1, 7.2	5.1, 7.1	5.1, 6.9
D77	~0, 9.4	0.1, 9.3	1.9, 10.8	1.3, 11.3	1.8, 11.0	1.5, 11.6
C80	9.6, 2.8	9.2, 3.4	12.2, 4.5	11.3, 4.9	11.5, 4.8	11.4, 4.7
S89	0.3,/	0.5,/	2.2,/	1.9, 2.3	1.9, 2.2	2.0, 2.3

Note. J_{opt} indicates the *J* value resulting in the best fit between simulated and experimental lines; J_{app}^{sim} indicates the apparent value of the *J*, obtained as explained in the text, from the simulated traces; J_{app}^{exp} indicates the apparent value of the *J*, obtained as explained in the text, from the experimental traces. The accord between the J_{app}^{exp} and the J_{app}^{sim} in each experiment supports the quality of the fit. The J_{opt} values are very close to those of J_{app}^{exp} for the DQ/ZQ-HCCH-E.COSY experiment, while larger differences are observed for the HCCH-E.COSY.

for the HCCH-E.COSY and ^{1}H magnetization of the CH_2 group for the DQ/ZQ-HCCH-E.COSY. Since with our version of the program it was not possible to define a spin system consisting of more than four spins, each of the two sequences was divided into two parts, the first one ending before the carbon mixing pulse ($C^1 \leftrightarrow C^2$ transfer) and the second one starting immediately after this pulse. In the HCCH-E.COSY experiment the spin system was defined as $H^1H^2C^2H^3$ in the first part of the experiment and as $H^1H^2C^1H^3$ in the second part; in the DQ/ZQ-HCCH-E.COSY experiment the other way around, because of transfer in the other direction. A starting density operator was defined in the Liouville operator space for each of the two different states of spin H^1: $\pm C_{2x} + 2C_{2x}H_{1z}$ for the HCCH-E.COSY and $\pm C_{1y}H_{2x} + 2C_{1y}H_{2x}H_{1z}$ for the DQ/ZQ-HCCH-E.COSY. The initial density operator evolved during each time interval under the action of a propagator defined by a Hamiltonian and a relaxation superoperator. The Hamiltonian included all the weak coupling terms and, only during acquisition, the chemical-shift terms; only spin–spin dipolar interactions were taken into account as effective relaxation mechanisms: the relaxation superoperator contained all the $J(0)$ terms of a fully correlated relaxation superoperator. For rhodniin a correlation time of 6 ns was used, according to what was found from ^{15}N relaxation measurements (M. Hennig, Diplomarbeit Universität Frankfurt/M). Additional auto-relaxation terms were added to the relaxation superoperator to account for possible dipole–dipole interactions between a nucleus of the spin system and other nuclei external to the spin system considered. Two trial values J_{trial} were originally assigned to the $^3J(H^{\alpha}, H^{\beta})$ and $^3J(H^{\alpha}, H^{\beta'})$ couplings and varied systematically until the simulated lines fitted with the experimental ones. The values for which the best fit between experimental and simulated lines was obtained are termed J_{opt}.

DISCUSSION

As can be seen in Fig. 8a for S89 the lineshape for the multiplet components in the HCCH-E.COSY experiment can be reproduced in the simulation. The outer lines, which correspond to the $\alpha(H^{\alpha})\beta(H^{\beta'})$ and $\beta(H^{\alpha})\alpha(H^{\beta'})$ states, relax faster than the inner ones, which correspond to the $\alpha(H^{\alpha})\alpha(H^{\beta'})$ and $\beta(H^{\alpha})\beta(H^{\beta'})$ states, and are therefore broader. The apparent coupling constant $J_{app}^{sim} = 0.5$ Hz, extracted from the simulated traces as explained for the experimental data (method (a) or (b) stated earlier) is much lower than the input one $J_{opt} = 2.2$ Hz. The J_{opt} is equal to the relative shift of the *maxima* of the corresponding lines, which cannot be determined accurately enough in the experimental spectra due to the presence of the noise. This result shows that, if more accurate values for the coupling constants are desired from an HCCH-E.COSY spectrum, a fitting procedure between experimental and theoretical data is necessary. The quality of the fit for S89 is shown in Fig. 8b. If the HCCH-E.COSY experiment is simulated without relaxation in all time intervals of the sequence including acquisition, the apparent coupling constant is equal to the real one. When relaxation is reintroduced in the different time intervals of the sequence, spurious terms, that are not filtered out by the phase cycle or by the gradients, are generated. Their existence during the acquisition period can either increase or diminish the apparent value of the coupling constant. The presence of relaxation in all the time intervals of the sequence results in J_{app}^{sim} values which are up to 3 Hz lower than the input ones. The action of differential relaxation in acquisition (*18–20*) accounts only for ~1.1 Hz^2/J of the observed effect, which is, for example, less than 10% for the $^3J(H^{\alpha}, H^{\beta})$ of C80.

Simulated traces for the DQ/ZQ-HCCH-E.COSY experiment are shown in Fig. 9a. Here, due to the restrictions on the

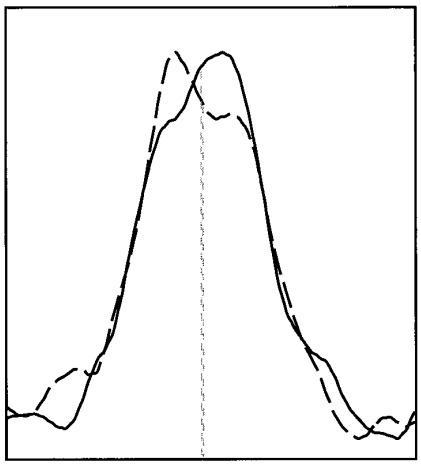

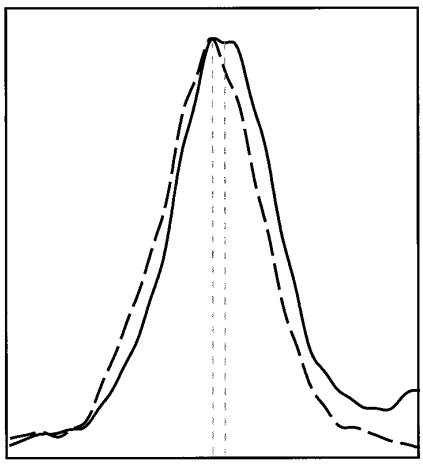

FIG. 7. Traces extracted in the ω_3 dimension from the ω_2-ω_3 plane corresponding to the H^{α} chemical shift of Ser89 in ω_1 of the 3D HCCH-E.COSY spectrum (a) and from the ω_1-ω_3 plane corresponding to the $H^{\beta'}$ chemical shift of Ser89 in ω_2 of the 3D-DQ/ZQ-HCCH-E.COSY spectrum (b). In (a) the traces correspond to the peak of Ser89 $\omega_1(H^{\alpha})$-$\omega_2(C^{\alpha})$-$\omega_3(H^{\beta})$; in (b) to the peak $\omega_1(C^{\beta})$-$\omega_2(H^{\beta'})$-$\omega_3(H^{\alpha})$. Both experiments were acquired on a 1.2 m*M* sample of the protein rhodniin. The HCCH-E.COSY experiment was performed on a Bruker DRX 600 spectrometer; the sweep widths were 8000 Hz (ω_1), 15380 Hz (ω_2), and 6120 Hz (ω_3); the acquired matrix consisted of $64(t_1) \times 102(t_2) \times 1024(t_3)$ complex points; the number of scans per increment was 4. The number of complex points in t_2 was extended to 204 by linear prediction; after Fourier transformation the size of the spectrum was reduced to 2640 Hz (ω_1), 3900 Hz (ω_2), and 4000 Hz (ω_3). The final zero-filled matrix had $128(\omega_1)$, $256(\omega_2)$, and $2048(\omega_3)$ complex points. The 3D DQ/ZQ-HCCH-E.COSY spectrum was acquired with the sequence of Fig. 5a on a Bruker DRX 800 spectrometer. The sweep widths were 16000 (ω_1), 6250 Hz (ω_2), and 8200 Hz (ω_3). The acquired matrix was $98(t_1) \times 128(t_2) \times 1024(t_3)$ complex points; each increment was acquired with 4 scans. The number of complex points in t_2 was extended to 155 by linear prediction; after zero-filling in all dimensions the resulting size of the matrix was $512(t_1) \times 256(t_2) \times 2048(t_3)$ complex points. The traces extracted from the HCCH-E.COSY spectrum were corrected for the incomplete suppression of non-connected transitions according to Ref. (*6*). All the traces were zero-filled to 16K. The value of the relative shift in ω_3 of the two sub-multiplets in each experiment is reported in the figure.

size of the spin system, not all the coupling partners of the H^{α} spin could be defined in the last part of the sequence and therefore it was not possible to reproduce exactly the sub-multiplet patterns. The simulated lines show neither the triplet nor the quadruplet structure present in the experimental lines. Nevertheless, the overall fit of the experimental data is good (Fig. 9b). The measured coupling constant (1.9 Hz) is very close to the input one J_{opt} (2.0 Hz), thus suggesting a higher reliability of the J_{app}^{exp} values extracted from this experiment with respect to those obtained from the HCCH-E.COSY spectrum.

It should be noted that an exact reproduction of the experimental lineshape in the simulation was not possible for all the signals, due to the restrictions on the spin system size and on the calculation time, which impeded a more complete description of relaxation.

In Table 1 a summary of the coupling constants extracted from the two experiments is presented. In the third and sixth columns the values J_{opt} obtained via fitting of experimental lines are reported; the accord between the HCCH-E.COSY values and the DQ/ZQ-HCCH-E.COSY ones is fairly good ($\Delta_{max} = 0.8$ Hz). This observation substantiates the reliability of the described fitting procedure in the extraction of coupling constant data. For comparison the J_{app} values are reported for both experimental and simulated spectra (J_{app}^{exp} and J_{app}^{sim}). The two sets of apparent coupling constants are in good accord with each other, showing that the values obtained from the experimental spectra are not heavily affected by errors deriving from overlap or low signal-to-noise ratio. As for the signal reported in Figs. 8 and 9, the J_{app} values obtained from the DQ/ZQ-HCCH-E.COSY experiment are very close to the J_{opt} ($\Delta_{max} = \pm 0.3$ Hz), while those extracted from the HCCH-E.COSY spectrum are systematically 2–3 Hz lower than the J_{opt}. No explanation of this observation is possible without taking relaxation rigorously into consideration in all the time intervals of each of the two experiments. Such a detailed and involved analysis is outside the scope of this paper.

In conclusion it can be asserted that the DQ/ZQ-HCCH-E.COSY J_{app} values are more accurate than the HCCH-E.COSY ones. Therefore, when accurate values of the coupling constants are expected without use of the suggested simulated/experimental fitting procedure, the DQ/ZQ-HCCH-E.COSY experiment is to be preferred.

The great advantage of the DQ/ZQ-HCCH-E.COSY with respect to the HCCH-E.COSY experiment consists in the possibility of extracting the four ^3J(H, H) couplings of CH_2-CH_2 groups directly from four corresponding E.COSY-type multiplets, consisting of only two components each. This proves particularly useful in the determination of the χ dihedral angles of protein side-chains. In Fig. 10 the four signals corresponding to the $C^{\gamma}H_2$-$C^{\delta}H_2$ group of Pro67 are shown. The experimental lines have been fitted with simulated ones according to the procedure described above. Due to the complexity of the scalar and dipole coupling topology it was not possible to reproduce perfectly the lineshape of

the experimental sub-multiplets. Nevertheless the quality of the fit is quite good. The extracted ^3J(H,H) values [$^3J(H^{\gamma},H^{\delta})$ = 7.4 Hz; $^3J(H^{\gamma},H^{\delta'})$ = 7.1 Hz; $^3J(H^{\gamma'},H^{\delta})$ = 3.4 Hz; $^3J(H^{\gamma'},H^{\delta'})$ = 7.4 Hz] are used in the proline ring conformational analysis, together with the four $^3J(H^{\beta/\beta'},H^{\gamma/\gamma'})$ and the two $^3J(H^{\alpha},H^{\beta/\beta'})$ couplings. The values of these couplings can be obtained from a 3D DQ/ZQ-HCCH-E.COSY in which the carbon–carbon defocussing delay has been optimized for a ^{13}C nucleus with two ^{13}C coupling partners (Fig. 5b). The conformational analysis relies on a modified

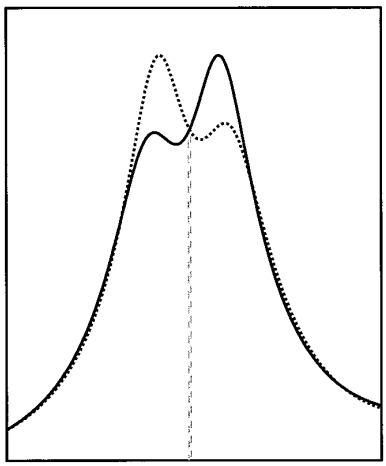

FIG. 8. In panel (a) the two simulated ω_3 traces corresponding to the low field (· · ·) and high field (—) component of the H^{α}, C^{α}, H^{β} peak of the HCCH-E.COSY experiment are shown. Their relative shift in the acquisition dimension is 0.5 Hz. The values for the coupling constants were $^3J(H^{\alpha},H^{\beta})$ = 2.2 Hz; $^3J(H^{\alpha},H^{\beta'})$ = 2.3 Hz; $^2J(H^{\beta},H^{\beta'})$ = −12 Hz, while the values of the distances between protons used in the simulation were $d(H^{\alpha},H^{\beta})$ = $d(H^{\alpha},H^{\beta'})$ = 2.52 Å; $d(H^{\beta},H^{\beta'})$ = 1.75 Å. The dihedral angles between the atoms pairs involved in the various dipole–dipole interactions have been derived assuming a χ_1 angle of −60°, as corresponding to two small $^3J(H^{\alpha},H^{\beta})$ and $^3J(H^{\alpha},H^{\beta'})$ couplings. In panel (b) the simulated traces from (a) have been superimposed on the experimental ones of Ser89 (- - - -; — — ·) to show the quality of the fit.

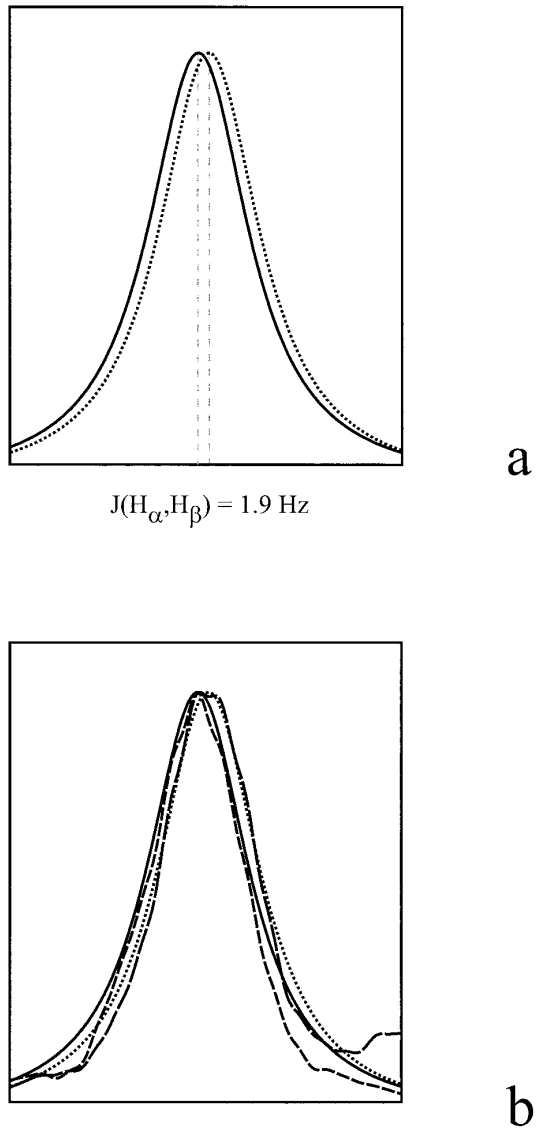

FIG. 9. In panel (a) the two simulated ω_3 traces corresponding to the low field (· · ·) and high field (—) component of the C^{β}, $H^{\beta'}$, H^{α} peak of the DQ/ZQ HCCH-E.COSY spectrum are shown. Their relative shift in the acquisition dimension is 1.9 Hz. The input values for the coupling constants were $^3J(H^{\alpha},H^{\beta})$ = 2.0 Hz; $^3J(H^{\alpha},H^{\beta'})$ = 2.3 Hz; $^2J(H^{\beta},H^{\beta'})$ = −12 Hz. The distances and dihedral angles values were derived as for Fig. 8. In panel (b) the simulated traces have been superimposed on the experimental ones of Ser89 (- - - -; — — ·) to assess the quality of the fit.

Karplus equation which relates ^3J(H, H) couplings constants and interproton dihedral angles θ (*16, 21–23*),

$$^3J_{HH} = a_1 \cos^2\theta + a_2\cos\theta + a_3 + \sum_i \Delta x_i'[a_4 + a_5\cos^2\xi_i\theta + a_6|\Delta x_i'|]. \quad [1]$$

The coefficients a_1–a_6 and ξ_i, as well as the values of the electronegativity difference Δx_i of the various HCCH

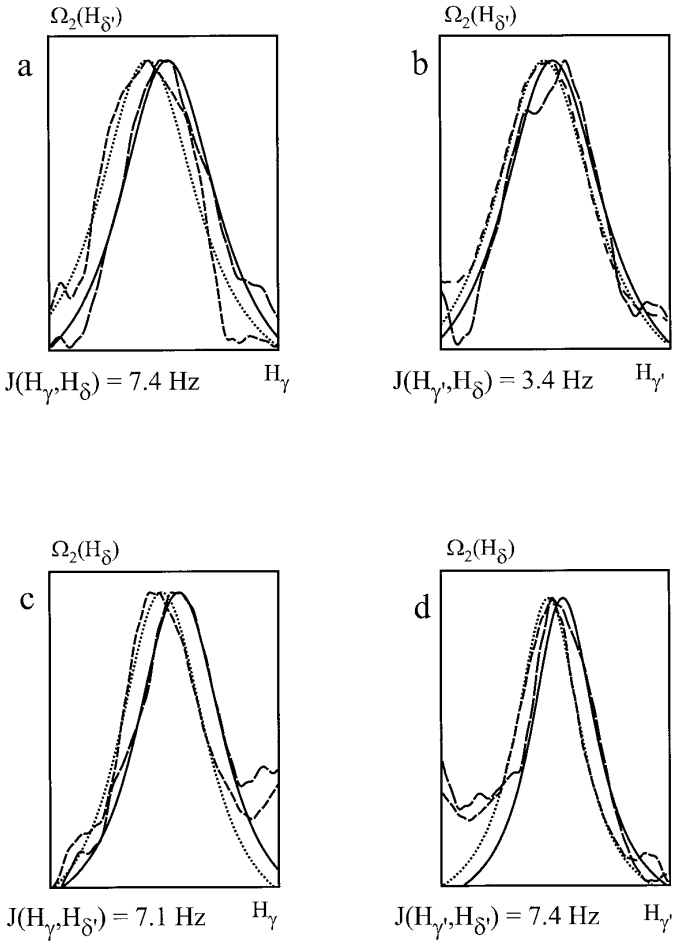

FIG. 10. Superposition of experimental (- - - -; — — ·) and simulated (· · · ; —) ω_3 traces for the four cross peaks of the $C^{\gamma}H_2$-$C^{\delta}H_2$ group of Pro67 in a DQ/ZQ-HCCH-E.COSY spectrum. The experimental traces have been extracted from ω_1-ω_3 planes; the nucleus whose chemical shift is recorded in ω_2 is reported on the top of each panel. The observed nucleus, as well as the J value for which the best fit between simulated and experimental lines was obtained, is reported below each panel. (a) C^{δ}, $H^{\delta'}$, H^{γ} peak; (b) C^{δ}, $H^{\delta'}$, $H^{\gamma'}$ peak; C^{δ}, H^{δ}, H^{γ} peak; C^{δ}, H^{δ}, $H^{\gamma'}$ peak.

fragment substituents with respect to hydrogen, are given in Ref. (*16*). A grid search is performed in the conformational space of the proline ring for each of the eight possible stereospecific assignments, varying systematically the pseudorotation phase P and the pseudorotation radius $\chi_{\max}$. For each conformation the vicinal coupling constants are calculated, based on Eq. [1] and compared with the experimental values (*16*). The r.m.s. deviation determines the quality of the fit. The experimental data can also be fitted with two dynamically interchanging ring conformations: the parameters of the grid search are then the two pseudorotation phases P_1 and P_2, the two pseudorotation radius $\chi_{\max,1}$ and $\chi_{\max,2}$ and the populations p_1 and $p_2 = 1 - p_1$ of the two conformations.

We tried to fit the four measured $^3J(H^{\gamma/\gamma'},H^{\beta/\beta'})$ with a two-conformations model. Since the four available coupling constants do not represent a sufficient number of constraints for a full conformational analysis of the proline ring, the $\chi_{\max,1}$ and $\chi_{\max,2}$ values were given a value of 40°, which is a value frequently found in such five-membered rings. The P_1 and P_2, as well as the populations of the two conformations, were left free. The best r.m.s. value (0.11) was found for the assignment $H^{\gamma} = H^{\gamma t}$; $H^{\delta} = H^{\delta c}$ or $H^{\gamma} = H^{\gamma c}$; $H^{\delta} = H^{\delta t}$ ($P_1 = 12.0$; $P_2 = 264.0$; $p_1 = 0.65$), while the epimeric assignment $H^{\gamma} = H^{\gamma c}$; $H^{\delta} = H^{\delta c}$ or $H^{\gamma} = H^{\gamma t}$; $H^{\delta} = H^{\delta t}$ gave an r.m.s. value of 0.39 ($P_1 = 216.0$; $P_2 = 364.0$; $p_1 = 0.50$). Thus the stereospecific assignment can be made based on the proposed method.

CONCLUSIONS

We have introduced a new experiment, the DQ/ZQ-HCCH-E.COSY, in which the four ^3J(H,H) coupling constants of CH_2-CH_2 groups can be measured directly from E.COSY-type multiplets consisting of only two components. The new experiment is particularly helpful for the determination of dihedral angles in protein side-chains. An example has been given for the Pro67 ring of the protein rhodniin.

A comparison between the ^3J(H, H) coupling constants in CH-CH_2 groups extracted from the new DQ/ZQ-HCCH-E.COSY and those obtained from a standard HCCH-E.COSY has been presented. For fast relaxing macromolecules, the need for a more sophistcated procedure of extraction of coupling constants, based on the fitting of experimental lines, has been demonstrated for the HCCH-E.COSY; for the DQ/ZQ-HCCH-E.COSY the difference between the apparent and true values of the J coupling constants is negligible in all the observed cases.

ACKNOWLEDGMENTS

This work was supported by the DFG (Gr 1211/2-4) and by the Fonds der Chemischen Industrie (A.R.). T.C. is supported by the E.U. through a Marie Curie stipend; H.S. is supported by the E.U. funded “Large Scale Facility for Biomolecular NMR in Frankfurt.”

REFERENCES

1. M. Karplus, *J. Chem. Phys.* **30,** 11 (1959).
2. M. Karplus, *J. Am. Chem. Soc.* **85,** 2870 (1963).
3. V. F. Bystrov, *Prog. NMR Spectrosc.* **10,** 41 (1976).
4. O. W. Sørensen, *J. Magn. Reson.* **90,** 433 (1990).
5. C. Griesinger and U. Eggenberger, *J. Magn. Reson.* **97,** 426 (1992).
6. H. Schwalbe, J. P. Marino, G. C. King, R. Wechselberger, W. Bermel, and C. Griesinger, *J. Biomol. NMR* **4,** 631 (1994).
7. U. Eggenberger, Y. Karimi-Nejad, H. Thüring, H. Rüterjans, and C. Griesinger, *J. Biomol. NMR* **2,** 583 (1992).
8. Y. Karimi-Nejad, J. M. Schmidt, H. Rüterjans, H. Schwalbe, and C. Griesinger, *Biochem.* **33,** 5481 (1994).
9. D. P. Zimmer, J. P. Marino, and C. Griesinger, *Magn. Reson. Chem.* **34,** S177 (1996).

10. C. Griesinger, O. W. Sørensen, and R. R. Ernst, *J. Am. Chem. Soc.* **107,** 6394 (1985).

11. C. Griesinger, O. W. Sørensen, and R. R. Ernst, *J. Chem. Phys.* **85,** 6387 (1986).

12. C. Griesinger, O. W. Sørensen, and R. R. Ernst, *J. Magn. Reson.* **75,** 474 (1987).

13. W. R. Croasmun and R. M. K. Carlson, "Two-Dimensional NMR Spectroscopy," pp. 569–571, VCH, New York (1994).

14. H. B. Olsen, S. Ludvigsen, and O. W. Sørensen, *J. Magn. Reson. A* **104,** 226 (1993); H. B. Olsen, S. Ludvigsen, and O. W. Sørensen, *J. Magn. Reson. A* **105,** 321 (1993).

15. J. M. Schmidt, O. W. Sørensen, and R. R. Ernst, *J. Magn. Reson. A* **109,** 80 (1994).

16. Z. L. Mádi, C. Griesinger, and R. R. Ernst, *J. Am. Chem. Soc.* **112,** 2908 (1990).

17. Z. L. Mádi and R. R. Ernst, wtest, personal communication.

18. G. S. Harbison, *J. Am. Chem. Soc.* **115,** 3026 (1993).

19. T. J. Norwood, *J. Magn. Reson. A* **104,** 106 (1993).

20. T. J. Norwood, *J. Magn. Reson. A* **101,** 109 (1993).

21. C. A. G. Haasnoot, F. A. A. M. de Leeuw, and C. Altona, *Tethraedron* **36,** 2783 (1980).

22. C. A. G. Haasnoot, F. A. A. M. de Leeuw, H. P. M. de Leeuw, and C. Altona, *Org. Magn. Reson.* **15,** 43 (1981).

23. C. A. G. Haasnoot, F. A. A. M. de Leeuw, H. P. M. de Leeuw, and C. Altona, *Biopolymers* **20,** 1211 (1981).